NASA Contractor Report 198209

A Concept for Transition Mapping on a 10°-Cone in the National Transonic Facility Using Flow-Pressure Variation

Ehud Gartenberg
Old Dominion University, Norfolk, Virginia

Contract NAS1-19858

September 1995

National Aeronautics and
Space Administration
Langley Research Center
Hampton, Virginia 23681-0001

Summary

A conceptual study was performed to define a technique for mapping the boundary-layer transition on a 10^0-cone in the National Transonic Facility (NTF) as a means of determining this cryogenic-tunnel suitability for laminar flow testing. A major challenge was to devise a test matrix using a fixed surface-Pitot probe, varying the flow pressure to produce the actual Reynolds numbers for boundary-layer transition. This constraint resulted from a lack of a suitable and reliable electrical motor to drive the probe along the cone's surface under cryogenic flow conditions.

The initial phase of this research was performed by the author in collaboration with the late Dr. William B. Igoe from the Aerodynamics Division at NASA Langley Research Center. His comments made during the drafting of this document were invaluable and a source of inspiration.

Table of Contents

Nomenclature

A	displacement amplitude of structural vibration
b.p.f.	blade passage frequency, =rps(fan)×25(=no. of blades)
a	acceleration amplitude of the fundamental frequency in the structural-vibration spectrum
f	value of the fundamental frequency in the structural-vibration spectrum
k	universal constant of transition length on a cone, =1-(x_t/x_T)=0.15
l	reference length of the cone, 44.5 inch, (1.130 meter)
M	Mach number
M.M.D.	Mach maximum deviation
M.S.D.	Mach standard deviation
p	pressure, measured with a steady-state transducer
p	instantaneous pressure, $p = \bar{p} + p'$
$\bar{p}$	average pressure
p'	pressure fluctuation
q	dynamic pressure in the test section
R	Reynolds number
T	temperature
T.M.D.	temperature maximum deviation
T.S.D.	temperature standard deviation
V	velocity
V.M.D.	velocity maximum deviation
V.S.D.	velocity standard deviation
x	distance along a cone ray from the cone apex
ϕ	phase of structural vibration

subscripts

$crest$	peak amplitude of an unsteady parameter
L	lower Reynolds number point of the measurement set
ne	never exceeded amplitude of an unsteady parameter
p	surface probe
s	flow static value
T	end of boundary-layer transition
t	flow total value, or beginning of boundary-layer transition
U	upper Reynolds number point of the measurement set
x	distance along a cone ray from the cone apex
∞	free-stream probe

Abbreviations

AEDC	Arnold Engineering and Development Center, U.S.A.
NASA	National Aeronautics and Space Administration, U.S.A.
NTF	National Transonic Facility at NASA Langley
ONERA	Office National de la Recherche Aerospatiale, France
RAE	Royal Aeronautical Establishment, U.K.
0.3M TCT	0.3M Transonic Cryogenic Tunnel at NASA Langley

1. Introduction

This report documents a conceptual study for the investigation of the flow quality in the National Transonic Facility (NTF), in terms of its capability to perform laminar flow testing at high-unit-Reynolds numbers. The study was performed in support of a cooperative program with a jet-engine manufacturer, who is interested in testing the model of its first laminar-flow nacelle for a large turbofan engine in the NTF.

The flow quality of the NTF, in terms of its fluctuating static pressure, was previously investigated by Igoe.[1] His results indicate that the flow quality in the NTF, when operated in air mode, is as good as, or better than, other wind tunnels of comparable size, which are renowned for their "quiet" flow (ref. 1, Fig. 47). This conclusion is particularly true for the transonic regime, where the NTF seems to have the "quietest" flow among its contemporaries. In addition, measurements made in the cryogenic mode did not indicate any perceptible difference in the level of pressure unsteadiness after the liquid nitrogen injection was cut-off (ref. 1, Fig. 52). The comparison between the NTF and other similar tunnels, and between the NTF's air and cryogenic modes of operation, yields encouraging indicators with respect to this tunnel's capability to allow laminar-flow testing at high unit-Reynolds numbers.

The extent of the laminar-boundary layer on 10^0-cones at zero angle of attack has been used for a long a time as an indication of a wind tunnel flow quality and its adequacy for laminar flow testing. Three detection techniques of the laminar boundary-layer transition to turbulence have been proven in cryogenic tunnels: unsteady pressure measurements (ref. 1, Fig. 24), infrared imaging,[2,3] and deposited hot films[4]. Both the IR technique and hot films were recently used with a 10^0-cone in a flow-quality investigation of a major wind tunnel at ONERA in France.[5] In the present case, however, a more traditional approach is recommended, in the form of unsteady pressure measurements made with a traversing-Pitot probe on the cone's surface, in analogy

1

with the "AEDC 10^0-cone." This technique was tested extensively in flight and in many of the major wind tunnels around the world,[6] and it can provide a uniform base of comparison of the flow quality of the NTF with respect to similar tunnels in the world. However, unlike the AEDC cone, the traversing probe of the NTF cone cannot benefit from the convenience of motorized positioning, because of a current lack of adequate and reliable electrical motors for operation in cryogenic tunnels. Therefore, the probe's position would have to be manually adjusted, and the Reynolds number at the probe's location would be adjusted by varying the unit-Reynolds number through the flow pressure.

Changing the unit Reynolds number through a corresponding change in the flow's pressure is a routine procedure in pressurized conventional and cryogenic wind tunnels. Furthermore, by running the test program at progressively higher unit Reynolds numbers, and successive shorter lengths of laminar flow, the measurements are performed with a presumably pristine upstream surface, unaffected by the traces left by the traversing probe, as was the case with the AEDC cone. On the negative side, this procedure generates flow unsteadiness when the pressure in the tunnel is changed, and noise is generated when the tunnel is vented to decrease the pressure.

A follow-up verification test with a shorter composite cone is recommended, in which IR imaging and deposited hot films should be used for transition detection. The results produced by the three experimental methods should be compared and used as evaluation criteria for transition measurements on aerodynamic models, on which traversing probes are impractical.

2. Determination of Test Conditions

The technique of mapping the transition process by varying the unit-Reynolds numbers, requires an *a priori* estimate of the tunnel pressure that would produce the transition Reynolds

number at the probe's position, assuming constant flow temperature and Mach number. Subsequently, the pressure range that produces the corresponding Reynolds-number range of the entire transition process can be calculated. To summarize this procedure:

1. Based on boundary-layer transition data on 10^0-cones, gathered in tunnels similar to the NTF, the transition Reynolds number as a function of the Mach number is estimated.

2. For a presumed transition occurrence in terms of Reynolds and Mach numbers, a temperature and probe location of interest are assumed and the corresponding flow pressure is deduced.

This philosophy is elaborated in what follows.

Figure 1 shows a typical change in the surface-Pitot pressure through the boundary-layer transition process on a 10^0-cone; x_t marks the start of transition coordinate, and x_T marks the end of transition coordinate. x_t is the end of the absolutely quiet laminar boundary layer, and will henceforth be called the transition point; x_T is the start of the fully developed turbulent boundary layer, and will be called the turbulence point, respectively. Figure 2 shows a similar plot, drawn in terms of the local Reynolds number, as well as the variation in the r.m.s. value of the static pressure. The start and the end of the transition Reynolds numbers are R_t and R_T respectively, and the value of the Reynolds-numbers interval over which the transition process develops is R_T-R_t, henceforth to be called "the interval". In this test plan, the measurements are planned to stretch across three intervals, to include one interval below R_t, and one interval beyond R_T. Hence, measurements are planned to be taken between R_t-(R_T-R_t) and R_T+(R_T-R_t). In terms of measurements taken at constant unit-Reynolds numbers, this Reynolds-number range is equivalent to the coordinate interval x_t-(x_T-x_t) and x_T+(x_T-x_t). To simplify the notation, the lower point Reynolds number of the measurement set, R_t-(R_T-R_t) is designated

R_L, and the upper point Reynolds number, $R_T+(R_T-R_t)$ is designated R_U. The values of other parameters at these two points are designated accordingly. To estimate numerical values of the transition development and the respective measurement sets, it is assumed that boundary-layer transition on slender cones does not have a characteristic length scale. Consequently, the boundary-layer transition data of Fig. 1, indicating the transition point at $0.61l$ and the turbulence point at $0.72l$ (l is the reference length of the cone), scales to all flow conditions, the proportionality constant k being

$$k = 1 - \frac{x_t}{x_T} \qquad (1)$$

$x_T/x_t{=}0.61/0.72{=}0.85$, and hence $k{=}0.15$, which is presumed to be a universal value on 10^0-cones. Consequently, $R_U{=}1.15R_T$, and $R_L{=}0.85{\times}0.85R_T{=}0.72R_T$, resulting in a measurement set between R_U and $R_L{=}0.72/1.15{=}0.63R_U$. Figure 3 plots the estimated boundary-layer turbulence point x_T vs. Mach number, at constant unit Reynolds number, while Fig. 4 plots the estimated turbulence point Reynolds-number, R_T vs. Mach number. This estimate is based on measurements on the AEDC 10^0-cone in NASA Langley's 8-Foot Transonic Pressure Tunnel,[7,8] albeit at lower unit-Reynolds numbers, and was adopted, as is, as a baseline for the NTF. Therefore, the combined information contained in Figs. 1 and 4, provides numerical estimates for R_T and R_t as a function of the Mach number. Based on this information and NTF performance charts, the test conditions of interest can be tabulated. For a given Mach number and total flow temperature, a probe location on the cone's ray can be assumed, for which R_U/ft and R_L/ft can be calculated. For these unit-Reynolds numbers, the corresponding total pressures $p_{t,U}$ and $p_{t,L}$ can be deduced, hence completing the calculation procedure for the NTF test conditions. Figure 5 gives a graphical representation of the estimated turbulence point x_T for various Mach numbers, as function of the unit-Reynolds number, for total pressures between 15 and 75 psia. Also indicated are the envelopes for x_L and x_U, that show the probe locations

4

that may cover most of the test conditions of interest. The actual test conditions in terms of total pressure, are constrained by the operational hard limits of the NTF: 15 psia minimum, 130 psia maximum. Power limitations further limit the pressure, according to the flow temperature and Mach number. In addition, it is customary to limit the cryogenic runs to 75 psia for operational reasons, e.g., the lack of adequate thermal capacities of primary component heaters, such as sidewall actuators and door locks, and the ability to make fast model changes in-between cryogenic runs.

3. Considerations for the Test Conditions

The first 13 runs (see Ch. 11) are planned to collect a minimal set of relevant data in the air mode. The rest of the runs were planned to have the probe moved progressively upstream, so that all the measurements are made on an undisturbed "pristine" cone surface. Probe and pressure-orifice positions are specified relative to the cone's apex, see Ch. 5.

3.1 Air Runs

Calibration runs P1 and Y1 will produce angle-of-attack sensitivity data, to allow the positioning of the cone at zero angle-of-attack in both pitch and yaw. The cone should be swept between -2^0 and $+2^0$, both in its normal position, and rolled 90^0 degrees around its axis, in increments of 0.1^0. Based on the differential pressure readings from the diametrically opposed orifices located at 36 inches, the necessary angle-of-attack adjustments can be made.

Calibration runs C1 and C2 (at 100^0 F) will track the transition progress with the surface pressure transducers only (at 18, 22, and 26 inches respectively), verified with the probe positioned at 30 inches.

Figure 5 indicates that locating the probe at 9 inches can cover all the runs of interest at low

unit Reynolds numbers. It is assumed that at low Mach numbers, up to 0.4, the heat exchanger can maintain a total temperature of 100^0 F (runs 1 through 4), while at Mach numbers above 0.5, the total temperature is assumed to be 120^0 F (runs 5 through 13). Runs 14 and 15 are designed to find the tunnel's ability to sustain long runs of laminar flow, between 39 down to 24 inches, which are generally considered as indicative of high flow quality. These probe positions may prove to be too optimistic, and position adjustments in the upstream direction may be required. Runs 16 through 18 (at 100^0 F), and 19 through 21 (at 120^0 F), are representative of high unit Reynolds number conditions in air. For these test conditions, the NTF runs out of power around Mach 0.7.

3.2 Nitrogen versus Air Runs

Runs 22 and 23 (at 100^0 F), and 24 (at 120^0 F), are designed to provide comparative transition values for air and nitrogen. The temperature should be adjusted slightly to match the velocities in air, and the pressure should be adjusted slightly to match the Reynolds number in air.

3.3 Identical Unit-Reynolds-Numbers Runs

"High-Pressure / High-Temperature" runs versus "Low-Pressure / Low Temperature" runs.

Air runs 25 (at 100^0 F) and 26 (at 120^0 F) produce at high pressures the same unit Reynolds number as cryogenic runs 35 and 36 (at -250^0 F) at low pressures.

3.4 IR Compatibility Runs

Cryogenic runs 27 through 30 (Mach numbers 0.2, 0.4, 0.6 and 0.8 at -100^0 F) are designed to provide comparative data for boundary-layer transition detection with the commercial IR imaging system, operating in the $8\text{-}12\mu$m wave band, and used in the Research Facilities Branch.

This system was previously tested with good results in the 0.3M Transonic Cryogenic Tunnel (0.3M TCT).[2,3]

3.5 Frequency Selectivity Runs

The frequency of dynamic flow phenomena is known to be sensitive to flow velocity, rather than to flow Mach number, as reflected in the formulation of Strouhal number. Cryogenic run 31 (at Mach 0.3 and -211° F) has velocity and Reynolds-number set identical to run 16, while run 32 (at Mach 0.2 and -250° F), has Mach and Reynolds numbers identical to run 16. The hypothesis is that for frequency selectivity to exist, runs 16 and 31 should have identical most amplified frequencies, while runs 16 and 32 could differ in this respect.

3.6 Cryogenic Runs

Runs 33 through 44, and 45 through 53 are cryogenic runs (-250° F), at low and high unit Reynolds respectively.

The expected transition signature on the steady-state pressure measurements planned for the cryogenic runs deserves special attention. As shown in Fig. 6, the capture area of the surface-Pitot tube may exceed the thickness of the laminar boundary-layer at high unit-Reynolds numbers, thus making it impossible to obtain the pressure variation shown in Fig. 1. In Fig. 6, the surface-Pitot tube was assumed to have an internal diameter of 0.005 inch, and a wall thickness of 0.002 inch. The expected transition region is demarcated by the lines indicating local Reynolds numbers of 5×10^6 and 10×10^6 respectively. Although the actual probe should be flattened, the overall picture cannot be changed significantly – the probe's diameter cannot be reduced for measurement-response reasons, and the wall's thickness cannot be reduced for practical reasons. In spite of this difficulty, the transition process and the turbulent point can still be detected analyzing the unsteady pressure measurement component, which should

capture well the characteristic vortical bursts (see Schlichting, Fig. 16.22, p. 481).[9] Referring to Fig. 6, a more significant drawing would show the dimensions of the surface-Pitot tube relative to the momentum thickness of the boundary layer, rather than the (thicker) velocity thickness, but this difference would not change neither the operational recommendation nor the conclusion.

3.7 Summary of Test Runs

57 runs are recommended, 27 in air and 30 in nitrogen, of which 27 will be at low temperatures. Of the air runs, four are pre-test calibration runs.

2 air runs at 100° F (calibration for zero angle-of-attack in pitch and yaw)

2 air runs at 100° F (calibration with surface transducers)

23 air runs at 100° F to 120° F (Mach and Reynolds sweeps)

3 N2 runs at 100° F to 120° F (nitrogen vs. air)

4 N2 runs at -100° F (IR compatibility)

1 N2 run at -211° F (velocity frequency selectivity)

22 N2 runs at -250° F (Mach and Reynolds sweeps)

4. Estimated Wind-Tunnel Occupancy Time

Each run should consist of approximately 60 points, 30 points taken twice, once varying the test conditions from low pressure / low Reynolds number to high pressure / high Reynolds number, followed by 30 points going in the opposite direction, from high pressure / high Reynolds number to low pressure / low Reynolds number. This procedure moves the transition front, first from downstream to upstream the probe, and then in reverse, from upstream to downstream the probe. Following this strategy, the transition is first identified, with the probe proba-

8

bly affecting the transition process, while in the second pass, unaffected data are taken, the probe being positioned downstream of the process. In the NTF, the duration of tunnel-pressure changes depends on the testing mode. In air mode, the tunnel-pressure change is approximately 1.0 psi/min; in nitrogen mode, it depends upon the fan power. For the purpose of obtaining a rough estimate of the occupancy time, each point is assumed to require an average 30 seconds, from the time the wind-tunnel control system is commanded to change the flow conditions to the desired test condition, to the completion of the data acquisition, storage, and display. Therefore, each run will consume approximately 30 minutes, and for approximately 60 runs (rounded up from 57 projected runs, including the calibration runs), the net data acquisition time will require 30 hours. Furthermore, because of the dynamic nature of this test (tunnel conditions continually changing), it is assumed that data will be taken only 50% of the "on-line" time, and therefore the net testing time will be 60 hours, or approximately 4 two-shifts days.

One model change is estimated to take two shifts, or one day, and the projected 10 position changes will require 10 days.

The installation and removal of the model is estimated at 4 shifts each, i.e., a total of 4 days, and the model check-out and angle-of-attack calibration is estimated at another two shifts, or one day. Therefore, the test-section occupancy time is estimated at four weeks, or one month.

5. Brief Description of the NTF 10^0-Cone

The proposed NTF 10^0-cone, shown in Fig. 7, is 44.5 inches (1.1303 meter) long. It is mounted straight on a sting extension that connects to the NTF support sting, and in turn to the NTF stub sting #1. To prevent flow separation at its base, the cone surface is smoothly continued with a fairing, approximately 70 inch (1.778 meter) long, that extends over the extension and support sting to the stub sting, rendering to this assembly a smooth, aerodynamic

shape. The traversing probe tube can be manually moved back-and-forth through a cylindrical hollow cap, which is mounted on a blade attached to the sting extension, approximately 10 inches (254 mm) downstream the cone base. The cap is fabricated of two longitudinal halves attached together with screws, that prevent relative motion between the tube and the cap by generating radial and friction forces. At its upstream end, the traversing probe is fitted with a head mounting for a lenticular blade support for the surface-Pitot tube, that is pressed against the cone surface. This layout allows the positioning of the surface-Pitot tube anywhere along the ray of the cone. At 4 inches (101.6 mm) above the surface-Pitot tube, the head mounting also has two free-stream tube probes, for total pressure reference measurements, and for unsteady pressure measurements.

The tip radius of the cone of 0.001 to 0.002 inches (0.025 to 0.050 mm) was sized based on spheres' critical Reynolds number of 200,000 (based on diameter), at which the boundary-layer undergoes transition at 90^0 with respect to the forward stagnation point (ref. 9, p. 17). At NTF's higher Reynolds-number capability of say, 400×10^6 per meter, transition will occur on a semi-sphere with a diameter of 0.5 mm, or approximately 0.02 inches. In this case, the need to eliminate the risk of transition suggests to specify a diameter one order of magnitude lower, i.e., 0.05 mm or 0.002 inches. Therefore, the radius specification of 0.002 inches includes a relaxation of the original criterion by a factor of two.

The surface roughness was deduced from experimental results produced by Feindt on roughness-induced transition (ref. 9, p. 541). His results indicate that the transition is insensitive to roughness, if its Reynolds number is kept underneath the critical value of 120, irrespective of the stream-wise location. In the NTF, this criterion translates into a roughness of 0.3×10^{-6} meter, or 12×10^{-6} inches, and therefore, a surface roughness of 0.1- to 0.2×10^{-6} meter, or approximately 3- to 5×10^{-6} inches, rms, seems to be both practical and acceptable.

Both the cone and the traversing arm are fabricated of Vascomax 200, a cryogenic-certified steel.

The NASA Langley technical drawings' numbers of this model are D1078105 through D1078113, D1078138 through D1078145, D1078438 through D1078440. The assembly drawing is D1078113.

6. Instrumentation

The instrumentation location is schematically shown in Fig. 8.

6.1 Traversing Probe

6.1.1 One free-stream steady total pressure probe, for reference and measurement.

6.1.2 One unsteady total pressure surface-Pitot tube, referenced to the free-stream steady total pressure.

6.1.3 One free-stream unsteady total total pressure probe referenced to the steady free-stream total pressure.

6.1.4 Two accelerometers, for pitch and yaw vibrations.

6.2 NTF

6.2.1 One (static) steady pressure tap in the plenum, for measurement and reference.

6.3 10^0-Cone

6.3.1 Three unsteady static pressure orifices, referenced to the plenum steady pressure, at 18,

22, and 26 inches.

6.3.2 Two perpendicular pairs of diametrically opposed orifices for differential pressure measurement at 36 inches, for angle of attack adjustment in pitch and yaw.

6.3.3 Four thermocouples, 90^0 apart, at 30 inches, flush with the surface.

6.3.4 Two accelerometers, for pitch and yaw vibrations.

The unsteady pressure transducers are Kulite CCQ-093.

The accelerometers are PCB 309A-M42.

The differential pressure transducers are Barocells.

The thermocouples are Copper-Constantan, gage 24.

7. NTF Wind-Tunnel Instrumentation

The Ruska's for total and static pressure have the following absolute range

p_t(psi)	p_s(psi)
150	150
100	100
50	50
30	30
	15

and solenoid valves are used to shift through various ranges.

The ΔMach system uses a Ruska for p_t, and a high accuracy Barocell differential gage for p_t-p_s, 20 psi auto-range, with lock-out option.

The pressure tube lengths for the differential gage are necessarily longer than those for the individual Ruska's (apparently at least for the total pressure side), so the tube lag problem may be greater for the ΔMach system than that for the standard system. It should be possible to see which system is least affected by lag problems during a simple pressure blow-down experiment.

Stagnation temperature is measured with a platinum resistance thermometer accurate within 0.05^0 K, and with a response time of 1 to 2 seconds.

8. Sizing of Transducers

For the surface pressure measurements, a 10 psi transducer (Endevco 8507-10M16) was completely satisfactory in the 10^0 conical fairing during the NTF dynamic calibration.[1] The highest $\Delta p'$ experienced at M=0.8 and maximum p_t was 0.427 psi(rms). If a crest factor of 3 is assumed, then a peak amplitude of about 1.28 psi(peak) could be expected. With a safety factor of 3, an amplitude of 3.8 psi is obtained, which nominally would round up to 5 psi, providing that a satisfactory reference pressure (a damped, but not too highly damped plenum say) is utilized. This does not exactly remove the steady-state component from the signal, because the average plenum pressure is slightly lower than free stream static, and the cone surface average static pressure is slightly above the free stream static pressure. However, barring use of a local cone surface average static pressure, the plenum pressure is probably the next best choice.

For the free stream fluctuating stagnation probe, data taken with the AEDC cone at M=0.7, indicates p_t'/p_t=1.5% in the worst case (or $p_t' = 0.015p_t$), and if a crest factor of 3 is again assumed, $p_{t,crest}' = 0.045p_t$, and again, if a safety factor of 3 is applied, $p_{t,ne}' = 0.135p_t$. Ac-

13

cordingly, a 15 psi transducer would be appropriate. However, with only 10 psi and 50 psi transducers available, and with a conservative safety factor of 3, it is likely that a 10 psi transducer is marginally adequate if a satisfactory total pressure reference is used to completely rule out any steady-state levels.

Surface total pressure probe on cone must be capable to measure both steady-state and fluctuating pressure components. In this case, either free stream total pressure or cone static pressure can be considered for a reference. For the steady-state pressure component, previous measurements with the AEDC cone shows $p'(rms)=7$ psf peak value for M=0.75, $p_t=1387$ psf, R=2.5×10^6/ft, p=1955 psf, and q=376 psf at $T_t=100^0$ F. Therefore, $p'/q=7/376=0.0186$, or of the order of 0.02 (transitional). For q=7000psf=48 psi, $p'=0.02(48)=1$ psi, and again with a crest factor of 3, and a safety factor of 3, $p'_{p,ne}=9$ psi. The steady-state component can range from near stagnation pressure to near free stream static pressure. The actual steady-state Δp level will depend on the choice of reference pressure. The best choice for the 10^0-cone in the NTF will probably be the free stream total pressure probe, located on the probe holder head. At high total pressure, the unit Reynolds number will be high and the surface probe will be located forward where the cone surface boundary layer will be very thin, and the cone surface probe will experience primarily total pressure. The only circumstance where the surface probe can experience near free stream static pressure will be when the probe is located far aft on the cone, where the boundary layer is thicker. These aft locations will only be used at low unit Reynolds numbers where both the stagnation pressure and the Mach number are low, and the difference between total and static pressure are small.

Notice: Both the steady-state and fluctuating components are additive and both vary in an unknown way with the chosen x-location for the probe. Although it cannot be proven, it is thought that the majority of the input comes from the steady-state component part of the signal, and this magnitude can be used to size the transducer ($p'_{p,ne}=9$ psi), provided that the

reference pressure p_t has been properly chosen.

It is concluded that the 10 psi transducer will be adequate for the cone surface static rms, and the cone surface total pressure probe. The free stream fluctuating stagnation pressure probe may be marginal with a 10 psi transducer, but it is considered a reasonable choice at this time.

9. Requirements for Data Acquisition, Processing, and Display

9.1 Aerodynamic Data

9.1.1 Wind-Tunnel Data

The wind tunnel and the cone instrumentation data will be acquired, processed, displayed and printed-out by the existing data acquisition system of the NTF.

The following are the requirements for data display:
Top of the page: Full date, test #, run #
Title: NTF 10^0-cone, Mode (air or nitrogen), On-line data
Point #, Time (hh,mm,ss).

9.1.1.1 Wind tunnel data:
M(x.xxx), V(ft/sec)(xxxx.), V(m/sec)(xxx.x), $T_t(^0$ F)(xxx.x), T_t(K)(xxx.x), p_t(psia)(xxx.xx), p_t(bar)(x.xxx), q(psia)(xx.xx), q(bar)(x.xxx), R/ft($\times 10^{(-6)}$)(xxx.x), R/m($\times 10^{-6}$)(xxx.x), $R_{x,p}$($\times 10^{-6}$)(xx.xx), b.p.f.(Hz)(xxx).
For points 1 through 30 and 31 through 60 of each run, the current deviation from the nominal value should be indicated, ΔM, ΔT_t, ΔV, in both units systems, in format (x.xx).
For points 1 through 30, and separately for points 31 through 60 of each run, the standard

deviation and maximum deviation should be estimated for M, V, and T_t, in % of the steady-state value. On the display, these values should be labeled M.S.D., M.M.D., V.S.D., V.M.D., T.S.D., T.M.D., in format (x.xx).

9.1.1.2 Angle-of-Attack Calibration

Numerical display:

Angle-of-attack(degrees)(x.xx), Δp of the two pairs of diametrically opposed orifices at 36 inches on the cone (psi)(xx.xx), and (bar)(x.xxx).

Graphical display:

Δp vs. angle-of-attack, for the data required above.

9.1.2 Probes data

Numerical display:

$\bar{p}_\infty$(psia)(xxx.xx), $\bar{p}_\infty$(bar)(x.xxx), $\bar{p}_p$(psia)(xxx.xx), $\bar{p}_p$(bar)(x.xxx), $\frac{\bar{p}_p}{\bar{p}_\infty}$(x.xxx), $p'_\infty rms/q$(x.xxx), $p'_p rms/q$(x.xxx).

Graphical display:

Five seconds of p_∞ and p_p, one underneath the other.

$\frac{\bar{p}_p}{\bar{p}_\infty}$(x.xxx) vs. $R_{x,p}(\times 10^{-6})$, $\frac{p'_p rms}{q}$(x.xxx) vs. $R_{x,p}(\times 10^{-6})$.

$\frac{p'_\infty rms}{q}$(x.xxx) vs. $R_{x,p}(\times 10^{-6})$.

Points 1 through 30 and 31 through 60 of the same run will be displayed on the same graphs but with distinct symbols.

9.1.3 Unsteady pressure surface data:

Numerical display:

The output of the transducers at 18, 22, and 26 inches respectively will be displayed as:

$\frac{p'_{18} rms}{q}$(x.xxx), $\frac{p'_{22} rms}{q}$(x.xxx), $\frac{p'_{26} rms}{q}$(x.xxx)

16

Graphical display:

Five seconds of p_{18}, p_{22}, and p_{26}, one underneath the other,

$\frac{p'_{18}rms}{q}$ vs. $R_{x,p}(\times 10^{-6})$(xx.xx),

$\frac{p'_{22}rms}{q}$ vs. $R_{x,p}(\times 10^{-6})$,

$\frac{p'_{26}rms}{q}$ vs. $R_{x,p}(\times 10^{-6})$.

Points 1 through 30 and 31 through 60 of the same run will be displayed on the same graphs but with distinct symbols.

9.2 Dynamic Structural Data

The cone and the probe are each fitted with two perpendicularly oriented accelerometers, to monitor vibrations in the pitch and yaw planes respectively. For each one of the planes, the following information will be acquired, processed and displayed:

Graphical display:

– 1 second of raw signal (time series, one underneath the other, full width of the display)

Numerical display:

– $\Delta f_{probe-cone}$; $\Delta \phi_{probe-cone}$; (side by side)

– A_∞ amplitude of probe vibration; A_{cone} amplitude of cone vibration; (side by side).

The vibration displacement amplitudes A can be calculated from

$$A = const \frac{a}{f^2} \tag{2}$$

where a is the acceleration amplitude of the fundamental frequency in the spectrum, and f is the value of the fundamental frequency. The constant should be defined as to obtain the zero-to-peak amplitude in millimeters.

The shield of the accelerometers' data-signal cable (connected to the A/D card) should be

17

electrically grounded at the power source only.

The cone and the probe should be checked for their fundamental vibration frequency (tapped with a percussion hammer), to rule-out coincidence with the fundamental frequency of the NTF's arc sector.

The power supplies should be checked that they produce the proper voltage required by the accelerometers, and that the shape of their signal is clean.

For temperature compensation, the reading of any of the cone's four thermocouples can be used.

10. References

1. Igoe, W.B., "Analysis of Fluctuating Static Pressure Measurements in a Large High Reynolds Number Transonic Cryogenic Wind Tunnel," D.Sc. Dissertation, George Washington University, Washington D.C., 1993, also NASA Technical Paper 3475, 1995.

2. Gartenberg, E., Johnson, W.G.,Jr., Wright, R.E.,Jr., Johnson, C.B. and Carraway, D.L., "Transition Detection in a Cryogenic Wind Tunnel Using Infrared Imaging," AIAA J., Vol. 30, No.2, February 1992, p. 444-446.

3. Gartenberg, E. and Wright, R.E.,Jr., "Boundary-Layer Transition Detection with Infrared Imaging Emphasizing Cryogenic Applications," AIAA J., Vol.32, No. 9, 1994, pp. 1875-1882, 1994.

4. Gartenberg, E., Scott, M.A. Martinson, S.D., and Tran, S.Q., "Boundary-Layer Transition Detection with Hot Films in Cryogenic Wind Tunnels," Proceedings of the Forth Triennal International Symposium on Fluid Control, Measurement and Flow Visualization (FLUCOME'94), Toulouse, France, August-September 1994, submitted to AIAA J.

5. Pelissier, C., "Determination de la Longueur de Transition dans la Soufflerie F1," ONERA Proces-Verbal D'Essais No. 1/8571 GY, May 1990.

6. Fisher, D.F. and Dougherty, N.S., "Flight and Wind-Tunnel Correlation of Boundary-Layer Transition on the AEDC Transition Cone," in AGARD Conference Proceedings No. 339 - Ground / Flight Test Techniques and Correlation, p. 5-1 to 5-25, October 1982, also NASA TM-84902, November 1982.

7. Credle, P., "The Evaluation of the Transition Reynolds Number and Acoustic Level in

the NASA-Langley Research Center 8-Foot Transonic Tunnel," Memo for Record, ARO, Inc, Arnold Air Force Station, Tennessee, July 2, 1971.

8. Dougherty, N.S.Jr. and Steinele, F.W., "Transition Reynolds Number Comparisons in Several Major Wind Tunnels," AIAA paper No. 74-627, July 1974.

9. Schlichting, H., Boundary-Layer Theory, McGraw-Hill, 7th ed, New-York 1979.

10. Mabey, D.G., "Boundary Layer Transition Measurements on the AEDC 10^0 Cone in Three RAE Wind Tunnels and Their Implications," Procurement Executive, Ministry of Defence, Aeronautical Research Council, R & M No.3821, London 1978.

11. Test Conditions

Comment: Runs P1 and Y1 should be run in increments of 0.1 degrees between -2 and +2 degrees angle of attack, with the cone in its nominal position, and with the cone rolled 90 degrees around its longitudinal axis.

Mode: Air   Probe Location: undetermined   Temperature: $T_t=100^0$ F
Pressure: p_t=undetermined,   M=undetermined,   R=undetermined

Comment: Runs C1 and C2 (Fig. 9) should be sampled every 0.1 psia. In run C2, the laminar regime may not reach the surface-Pitot probe; see also runs 14 and 15.

Mode: Air   Probe Location: x_p=30.00 inch   Temperature: $T_t=100^0$ F

Run	M	R_U/ft $\times 10^{-6}$	R_L/ft $\times 10^{-6}$	$p_{t,U}$ (psia)	$p_{t,L}$ (psia)	Δp (psia)
C1	0.10	3.15	0.99	72.8	22.9	49.9
C2	0.20	3.15	1.24	37.5	14.8	22.7

Comment: All runs sampled 30 points at equal pressure intervals.

Runs 1 through 21 see Fig. 10.

Mode: Air   Probe Location: x_p=9.00 inch   Temperature: T_t=100^0 F

Run	M	R_U/ft $\times 10^{-6}$	R_L/ft $\times 10^{-6}$	$p_{t,U}$ (psia)	$p_{t,L}$ (psia)	Δp (psia)
1	0.10	5.25	3.30	121.3	76.4	45.0
2	0.20	5.25	3.30	62.5	39.3	23.2
3	0.30	5.25	3.30	42.7	26.9	15.8
4	0.40	5.25	3.30	32.3	20.3	12.0

Mode: Air   Probe Location: x_p=9.00 inch   Temperature: T_t=120^0 F

Run	M	R_U/ft $\times 10^{-6}$	R_L/ft $\times 10^{-6}$	$p_{t,U}$ (psia)	$p_{t,L}$ (psia)	Δp (psia)
5	0.50	5.28	3.32	27.9	17.6	10.4
6	0.60	5.40	3.40	25.3	15.9	9.4
7	0.70	5.80	3.65	24.7	15.6	9.2
8	0.75	6.07	3.82	25.2	15.9	9.3
9	0.80	6.36	4.00	25.4	16.0	9.4
10	0.85	6.68	4.20	26.0	16.4	9.6
11	0.90	7.01	4.41	25.9	16.3	9.6
12	1.00	7.74	4.87	27.7	17.4	10.3
13	1.05	8.14	5.12	28.7	18.0	10.6

Mode: Air   Probe Location: x_p=39.00 inch   Temperature: T_t=100° F

Comment: x_p may request forward adjustments if the laminar boundary layer transitions to turbulence at upstream location.

Run	M	R_U/ft $\times 10^{-6}$	R_L/ft $\times 10^{-6}$	$p_{t,U}$ (psia)	$p_{t,L}$ (psia)	Δp (psia)
14	0.10	1.21	.762	28.0	17.6	10.4

Mode: Air   Probe Location: x_p=24.00 inch   Temperature: T_t=100° F

Comment: x_p may request forward adjustments if the laminar boundary layer transitions to turbulence regime at upstream location.

Run	M	R_U/ft $\times 10^{-6}$	R_L/ft $\times 10^{-6}$	$p_{t,U}$ (psia)	$p_{t,L}$ (psia)	Δp (psia)
15	0.20	1.97	1.24	23.4	14.8	8.7

Mode: Air   Probe Location: x_p=4.50 inch   Temperature: T_t=100^0 F

Run	M	R_U/ft $\times 10^{-6}$	R_L/ft $\times 10^{-6}$	$p_{t,U}$ (psia)	$p_{t,L}$ (psia)	Δp (psia)
16	0.20	10.50	6.61	125.0	78.7	46.3
17	0.30	10.50	6.61	85.4	53.7	31.7
18	0.40	10.50	6.61	64.6	40.6	23.9

Mode: Air   Probe Location: x_p=4.50 inch   Temperature: T_t=120^0 F

Run	M	R_U/ft $\times 10^{-6}$	R_L/ft $\times 10^{-6}$	$p_{t,U}$ (psia)	$p_{t,L}$ (psia)	Δp (psia)
19	0.50	10.56	6.64	55.9	35.2	20.7
20	0.60	10.80	6.80	50.6	31.8	18.8
21	0.70	11.59	7.30	49.5	31.1	18.3

Comment: Nitrogen runs 22, 23, and 24 vs. air runs 16, 18 and 20. Match M,R,V. Adjust T slightly to match velocities in air, adjust p slightly to match the Reynolds number in air.

Runs 22 through 24, see Fig. 11, lower three bars.

Mode: Nitrogen   Probe Location: x_p=4.50 inch   Temperature: T_t=100^0 F

Run	M	R_U/ft $\times 10^{-6}$	R_L/ft $\times 10^{-6}$	$p_{t,U}$ (psia)	$p_{t,L}$ (psia)	Δp (psia)
22	0.20	10.50	6.61	125.0	78.7	46.3
23	0.40	10.50	6.61	64.6	40.6	23.9

Mode: Nitrogen   Probe Location: x_p=4.50 inch   Temperature: T_t=120^0 F

Run	M	R_U/ft $\times 10^{-6}$	R_L/ft $\times 10^{-6}$	$p_{t,U}$ (psia)	$p_{t,L}$ (psia)	Δp (psia)
24	0.60	10.80	6.80	50.6	31.8	18.8

Comment: Runs 25 and 26 (air) should be compared with runs 35 and 36 (cryo).

Runs 25 and 26, see Fig. 11, upper two bars.

Mode: Air   Probe Location: x_p=2.25 inch   Temperature: T_t=100° F

Run	M	R_U/ft $\times10^{-6}$	R_L/ft $\times10^{-6}$	$p_{t,U}$ (psia)	$p_{t,L}$ (psia)	Δp (psia)
25	0.40	20.99	13.21	129.1	81.3	47.9

Mode: Air   Probe Location: x_p=2.25 inch   Temperature: T_t=120° F

Run	M	R_U/ft $\times10^{-6}$	R_L/ft $\times10^{-6}$	$p_{t,U}$ (psia)	$p_{t,L}$ (psia)	Δp (psia)
26	0.50	21.12	13.29	111.8	70.3	41.4

Comment: Runs 27 through 30 (Fig. 12) provide compatibility data with commercial infrared imaging systems.

Mode: Nitrogen   Probe Location: x_p=4.50 inch   Temperature: T_t=-100^0 F (200K)

Run	M	R_U/ft $\times 10^{-6}$	R_L/ft $\times 10^{-6}$	$p_{t,U}$ (psia)	$p_{t,L}$ (psia)	Δp (psia)
27	0.20	10.50	6.61	68.6	43.2	25.4
28	0.40	10.50	6.61	35.7	22.4	13.2
29	0.60	10.80	6.80	26.6	16.8	9.9
30	0.80	12.72	8.00	26.2	16.5	9.7

Comment: Runs 16, 31 and 32 verify the velocity influence on frequency selectivity (if any). Runs 16 and 31 have identical velocities and Reynolds-number sets, at different temperatures and Mach numbers; $T_2=(\frac{M_1}{M_2})^2 T_1$.

Runs 16 and 32 have identical Mach numbers and Reynolds-number sets, at different temperatures.

Runs 31 through 53, see Fig. 13.

Mode: Nitrogen   Probe Location: x_p=4.50 inch   Temperature: T_t=-211° F

Run	M	R_U/ft $\times 10^{-6}$	R_L/ft $\times 10^{-6}$	$p_{t,U}$ (psia)	$p_{t,L}$ (psia)	Δp (psia)
31	0.30	10.50	6.61	28.05	17.6	10.45

Mode: Nitrogen   Probe Location: x_p=4.50 inch   Temperature: T_t=-250° F

Run	M	R_U/ft $\times 10^{-6}$	R_L/ft $\times 10^{-6}$	$p_{t,U}$ (psia)	$p_{t,L}$ (psia)	Δp (psia)
32	0.20	10.50	6.61	31.8	20.0	11.8

28

Mode: Nitrogen   Probe Location: x_p=2.25 inch   Temperature: T_t=-250^0 F

Run	M	R_U/ft $\times 10^{-6}$	R_L/ft $\times 10^{-6}$	$p_{t,U}$ (psia)	$p_{t,L}$ (psia)	Δp (psia)
33	0.20	20.99	13.21	63.6	40.0	23.6
34	0.30	20.99	13.21	43.4	27.3	16.1
35	0.40	20.99	13.21	32.9	20.7	12.2
36	0.50	21.12	13.29	27.4	17.2	10.2
37	0.60	21.60	13.59	24.3	15.3	9.0
38	0.70	23.19	14.59	23.6	14.8	8.7
39	0.75	24.28	15.28	23.5	14.8	8.7
40	0.80	25.44	16.01	24.1	15.2	8.9
41	0.85	26.71	16.81	24.3	15.3	9.0
42	0.90	28.05	17.65	24.7	15.6	9.2
43	1.00	30.97	19.49	26.3	16.5	9.7
44	1.05	32.56	20.49	27.2	17.1	10.1

Mode: Nitrogen   Probe Location: x_p=0.75 inch   Temperature: T_t=-250^0 F

Run	M	R_U/ft $\times 10^{-6}$	R_L/ft $\times 10^{-6}$	$p_{t,U}$ (psia)	$p_{t,L}$ (psia)	Δp (psia)
45	0.50	63.35	39.86	82.2	51.7	30.5
46	0.60	64.81	40.78	73.0	45.9	27.1
47	0.70	69.56	43.77	70.7	44.5	26.2
48	0.75	72.84	45.84	70.5	44.4	26.1
49	0.80	76.31	48.02	72.3	45.5	26.8
50	0.85	80.14	50.43	73.0	45.9	27.1
51	0.90	84.16	52.96	74.1	46.7	27.5
52	1.00	92.92	58.47	78.9	49.6	29.2
53	1.05	97.67	61.46	81.7	51.4	30.3
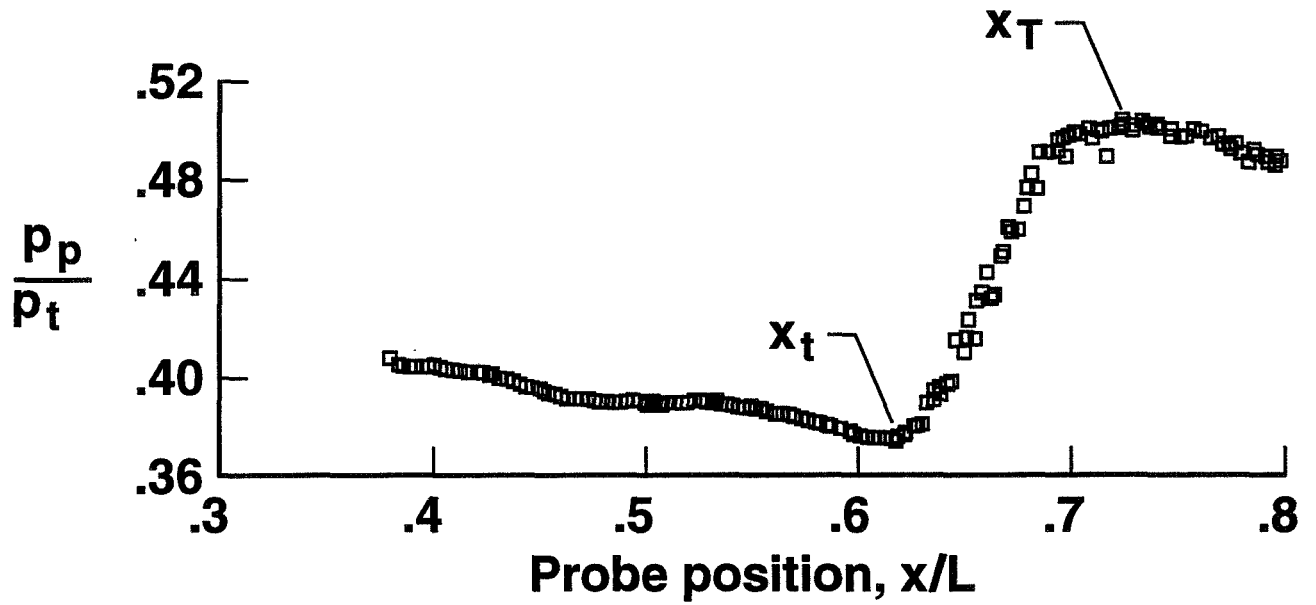
Figure 1: Typical pressure distribution through the boundary-layer transition process, measured in flight on the AEDC 10^0-cone with a surface-Pitot probe.[6] $M_\infty=1.44$, alt.=13,074m, $R=9.45\times10^6$/m.
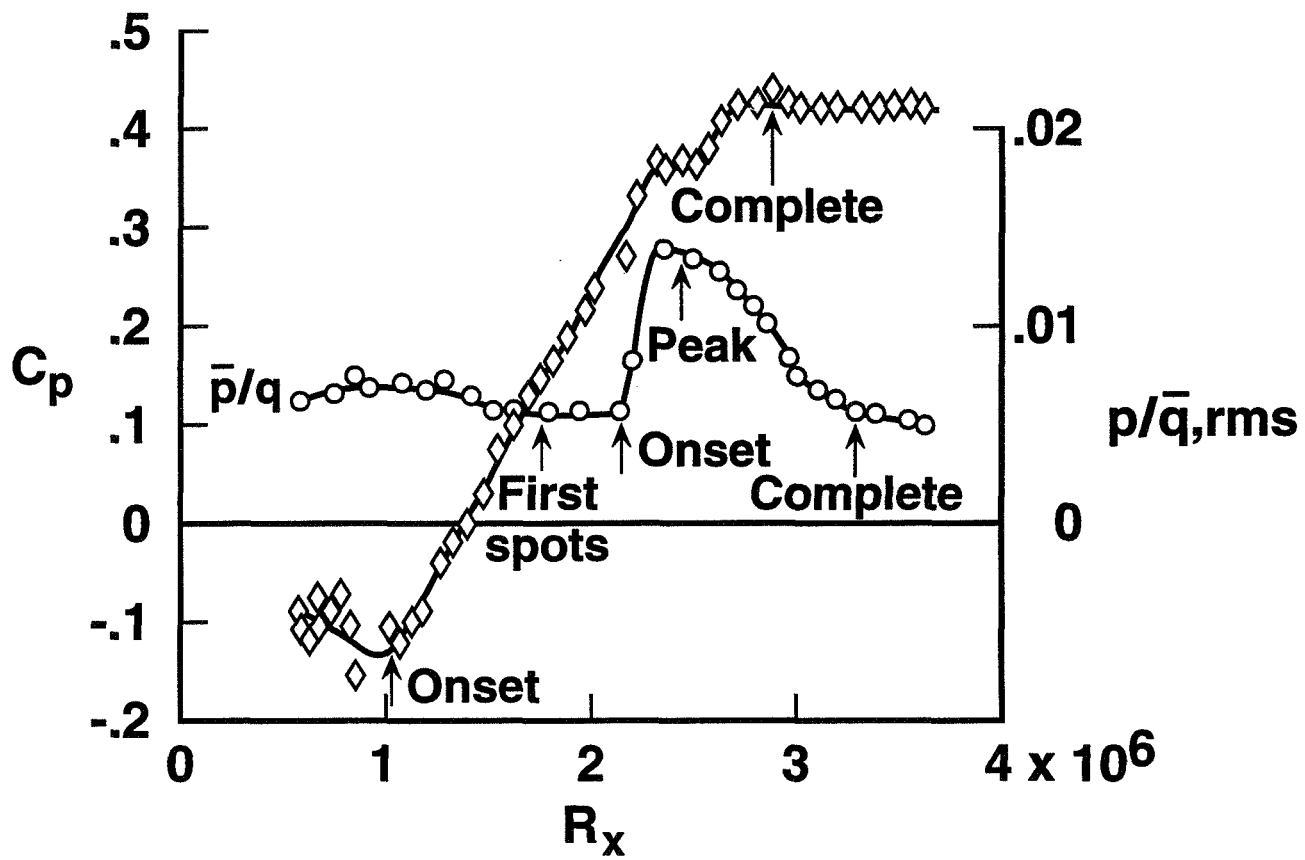
Figure 2: Comparison of boundary-layer transition static pressure fluctuations and fixed surface-Pitot pressure measured on the AEDC 10^0-cone in the RAE 8-ft×6-ft wind tunnel.[10] x=457mm, M=0.30.
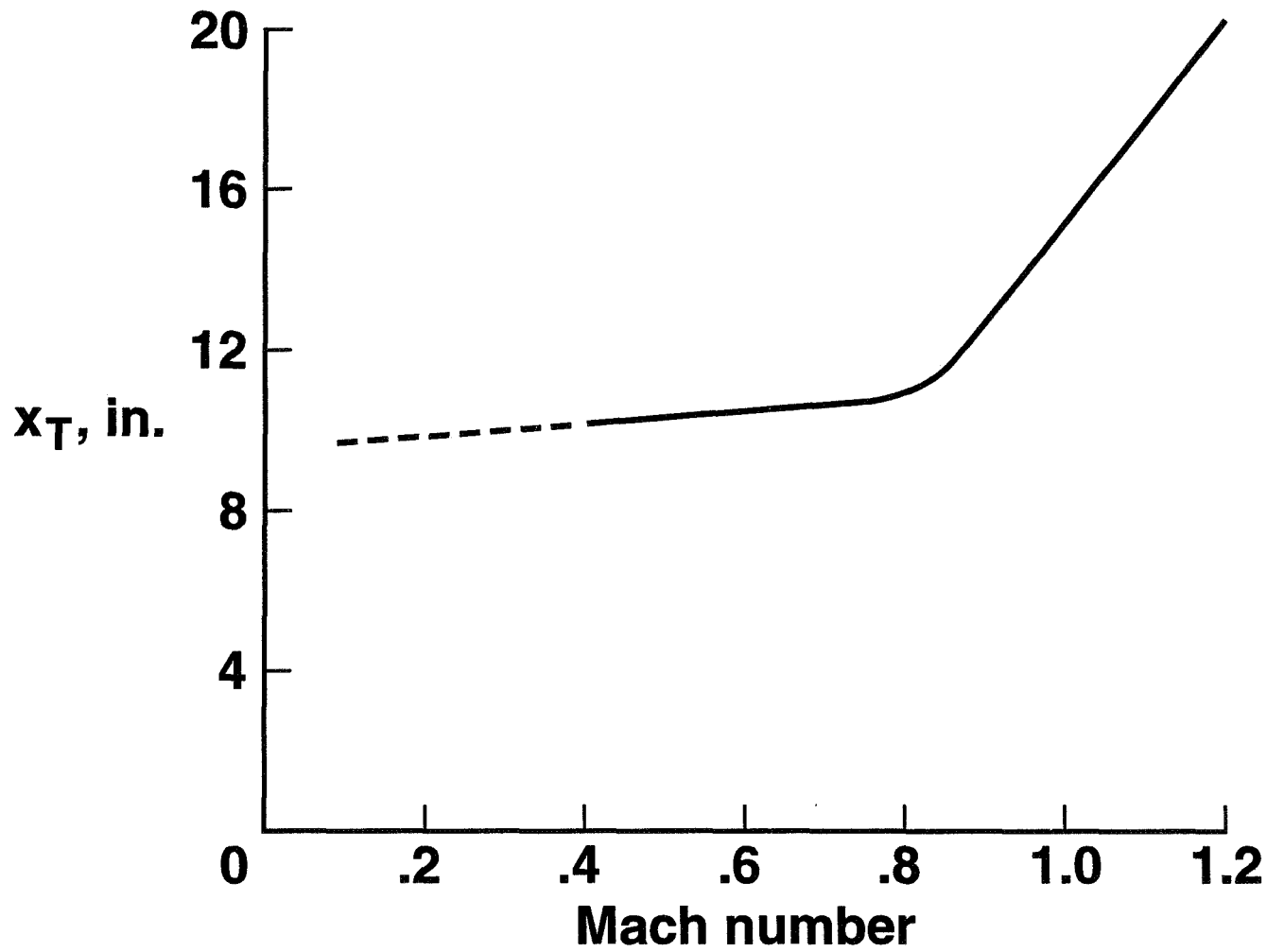
Figure 3: Estimated end of transition length as a function of the Mach number on a 10^0-cone in the NTF. $R=4\times10^6$/ft.
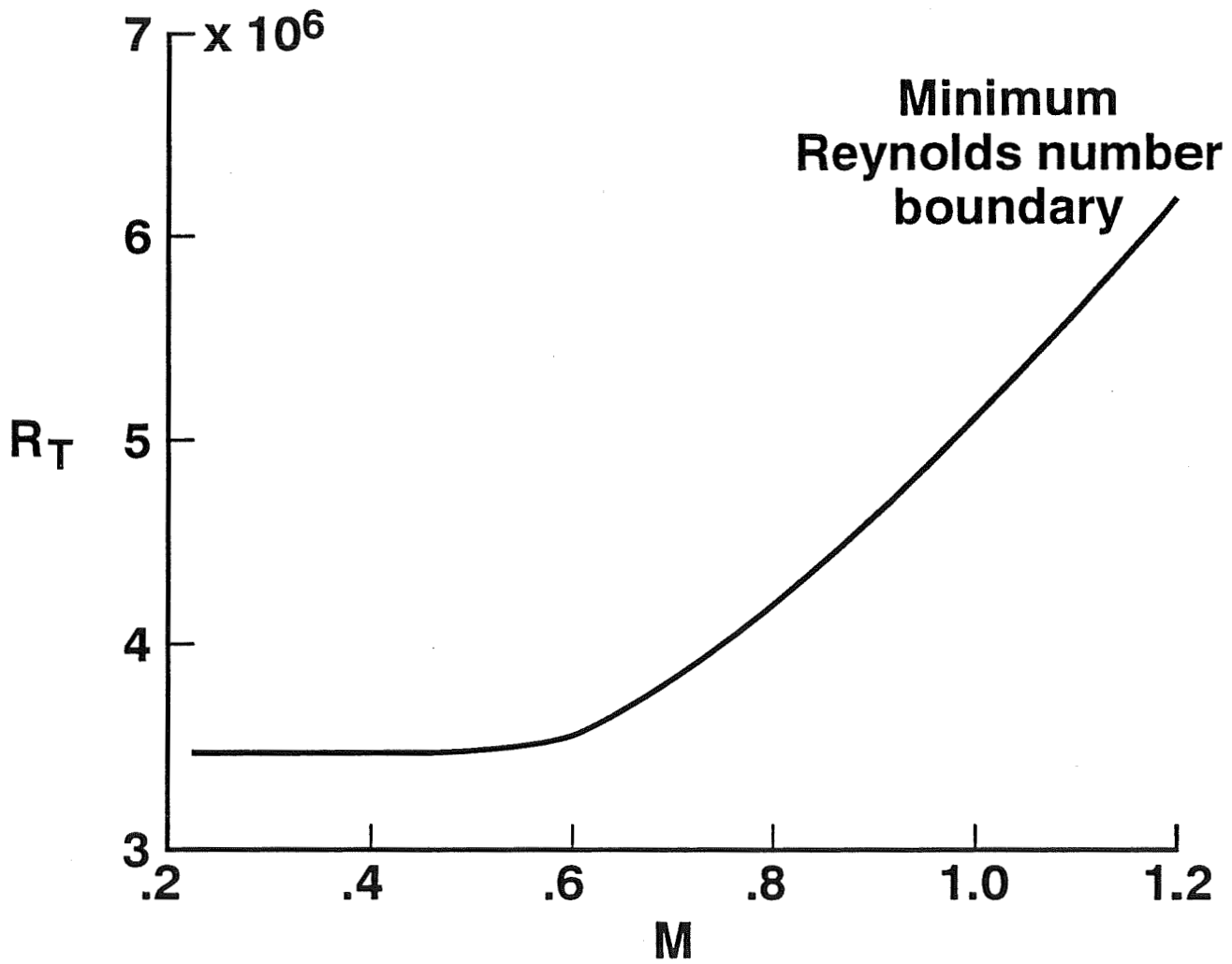
Figure 4: Estimated end of transition Reynolds number as a function of the Mach number on a 10^0-cone in the NTF.
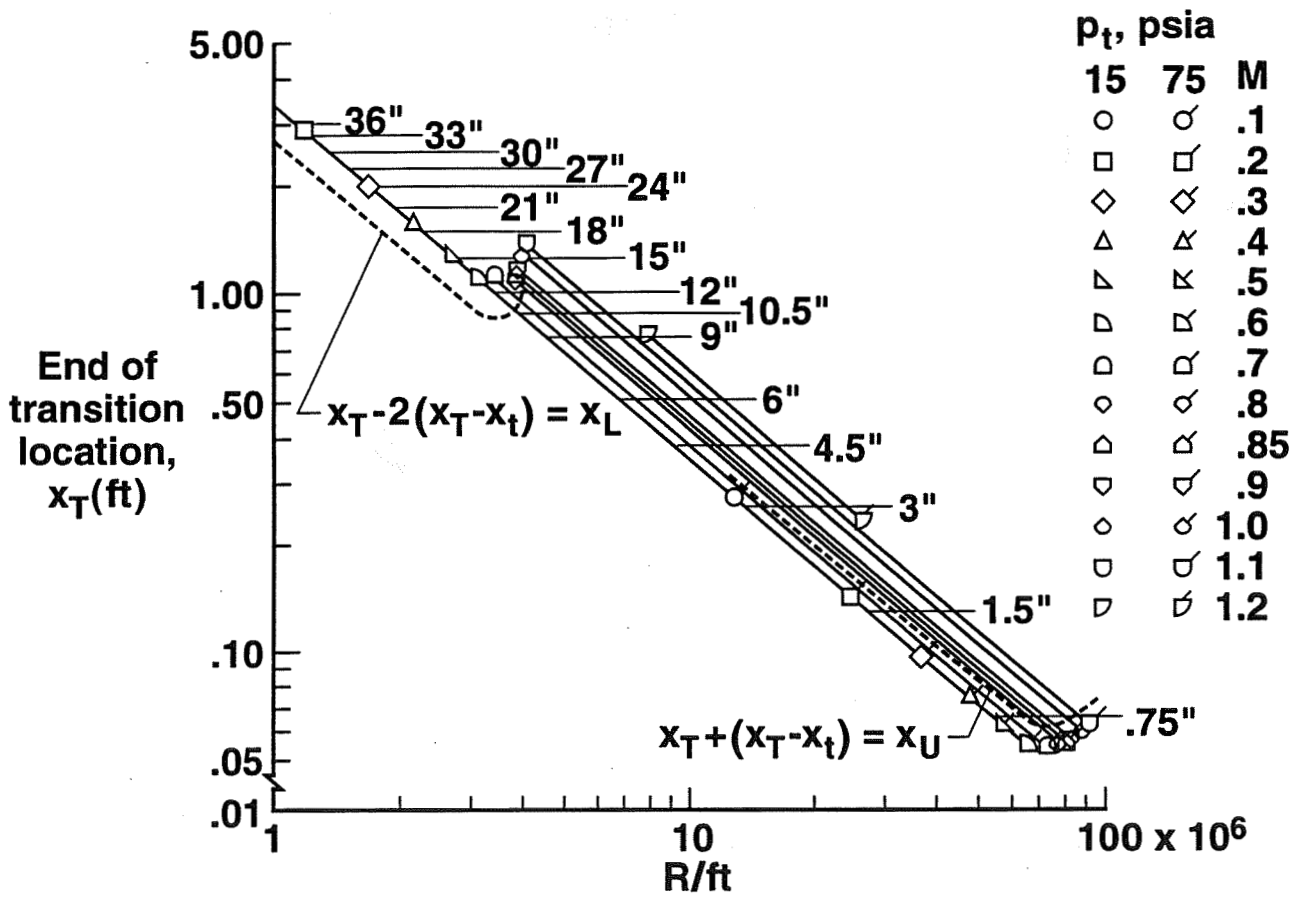
Figure 5: Estimated end of transition length as a function of the unit-Reynolds number on a 10^0-cone in the NTF, assuming $R_T = f(M)$.
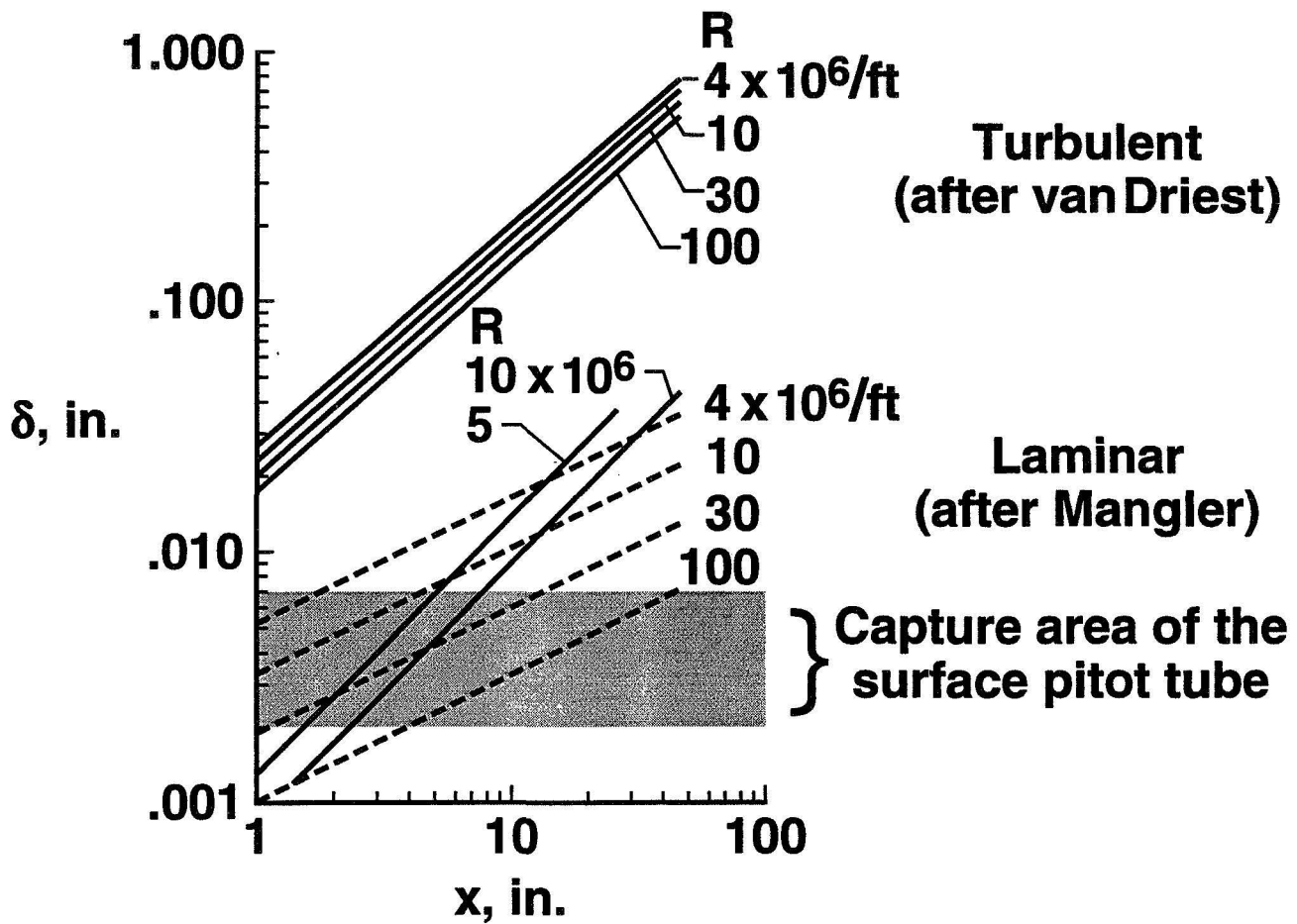
Figure 6: Incompressible boundary-layer thickness on a 10^0-cone.
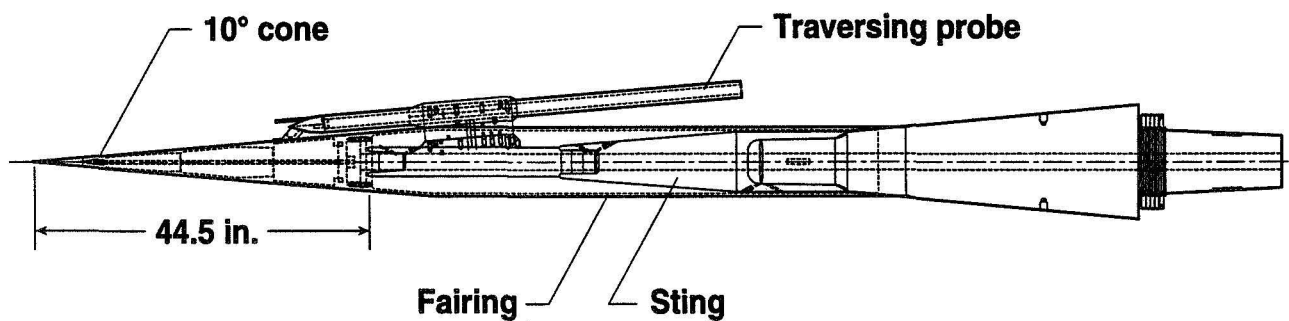
Figure 7: Schematics of the proposed NTF 10^0-cone.
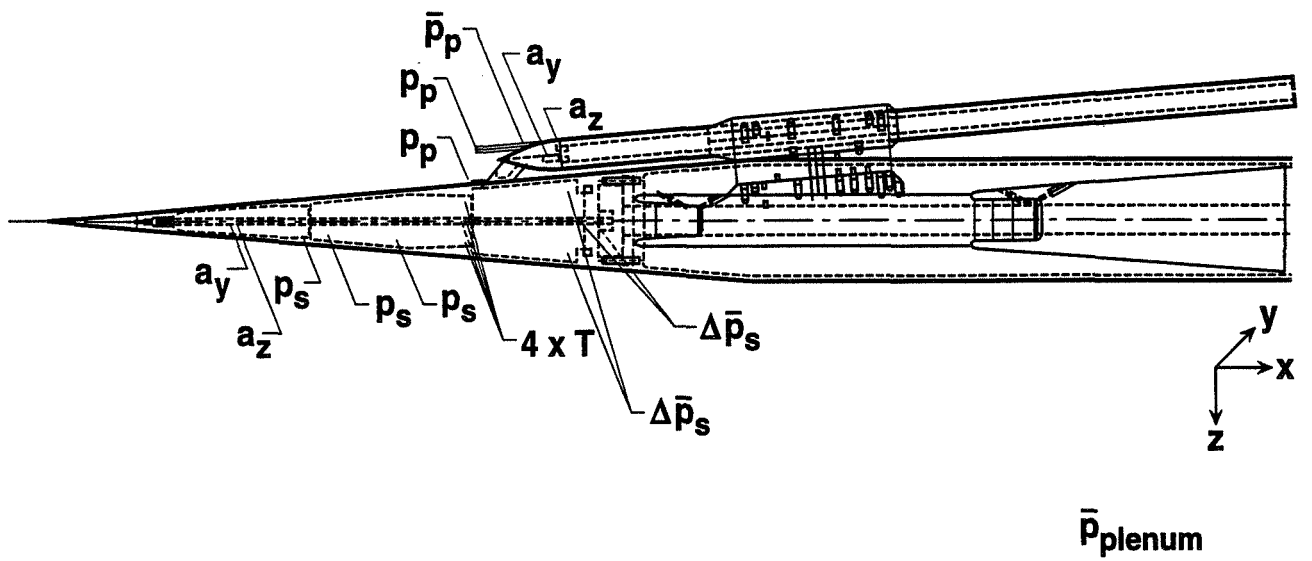
Figure 8: Schematics of the instrumentation for the proposed NTF 10^0-cone.
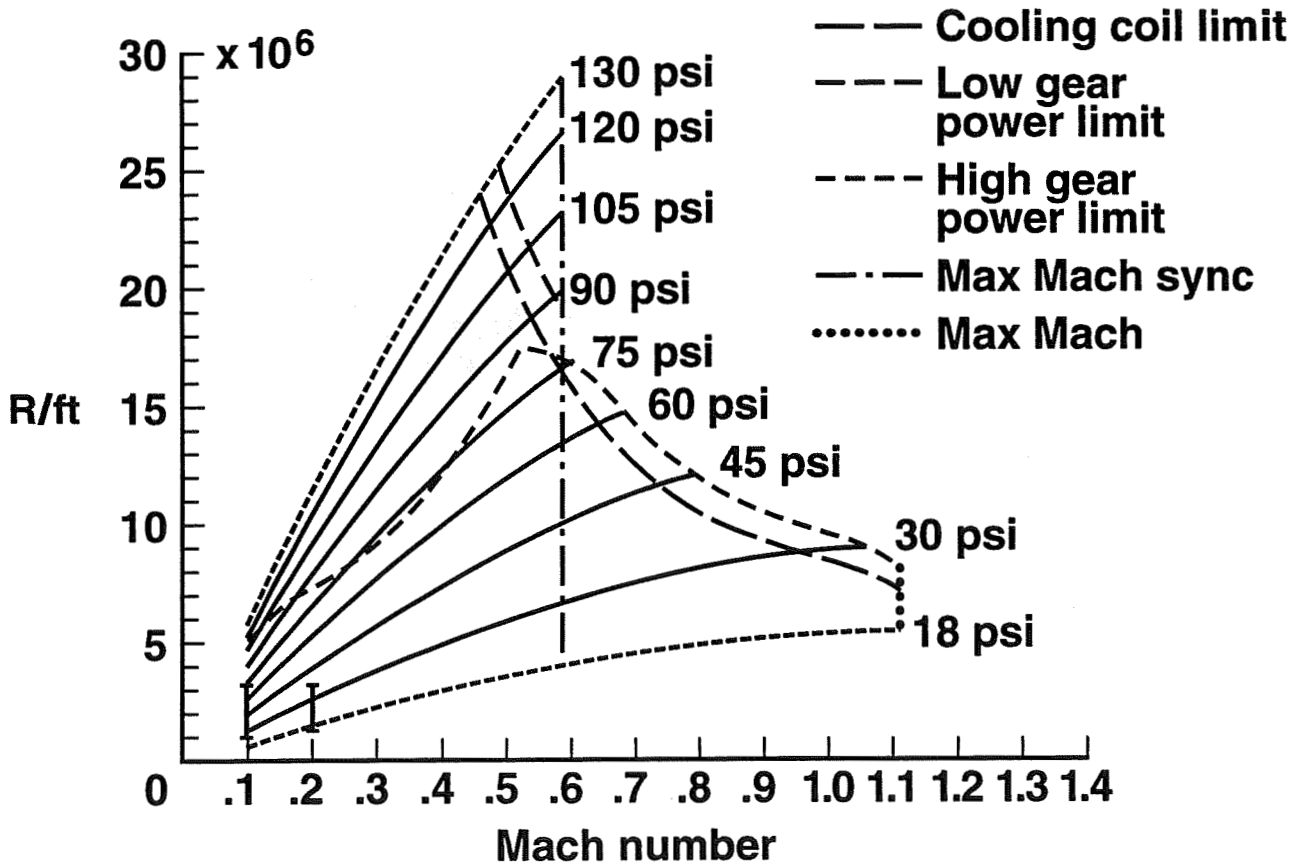
Figure 9: Proposed test plan for the NTF 10^0-cone. Air mode at 100^0 F, calibration runs C1 and C2 for surface pressure transducers.
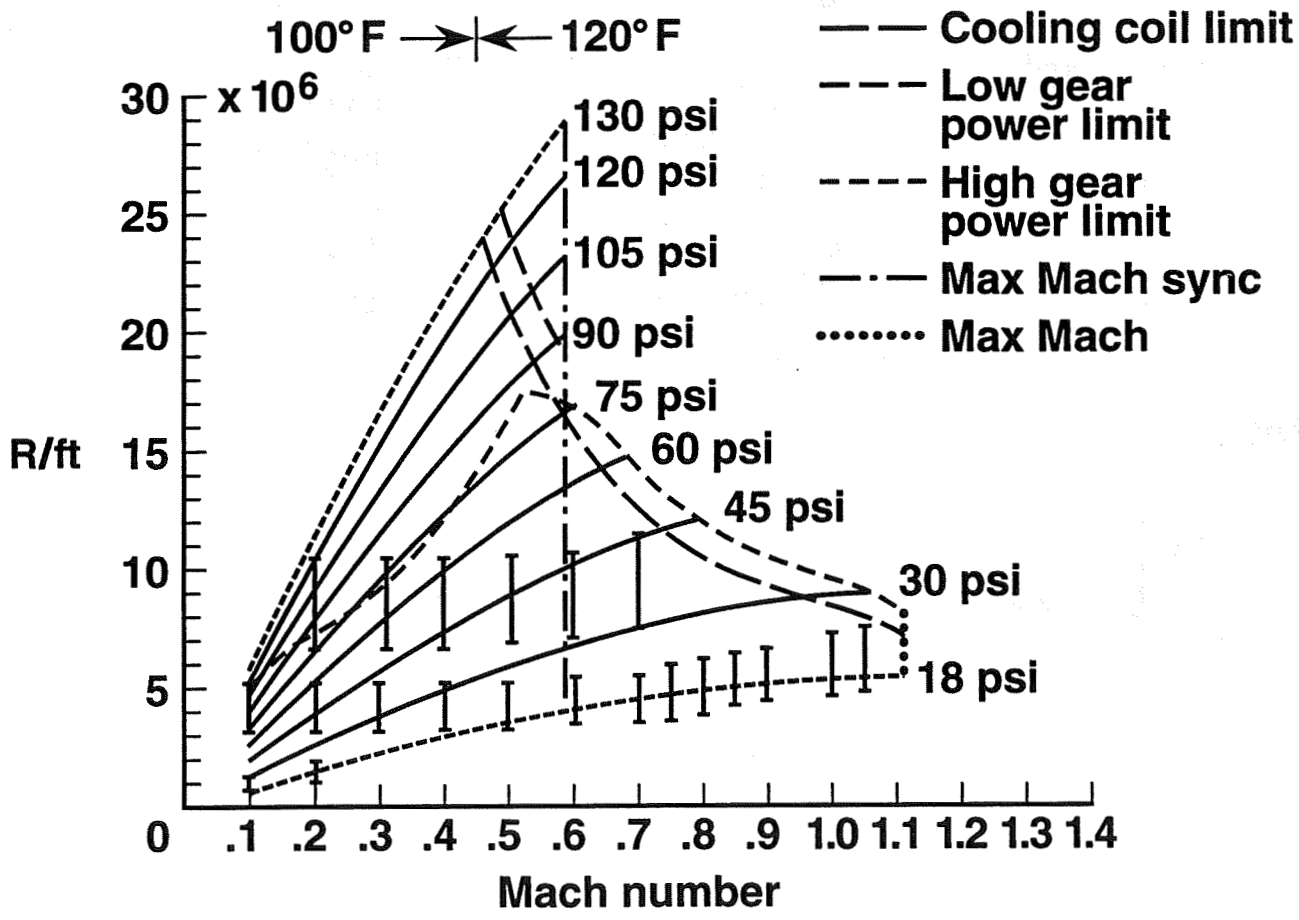
Figure 10: Proposed test plan for the NTF 10^0-cone. Air mode at ambient temperatures, runs 1 through 21.
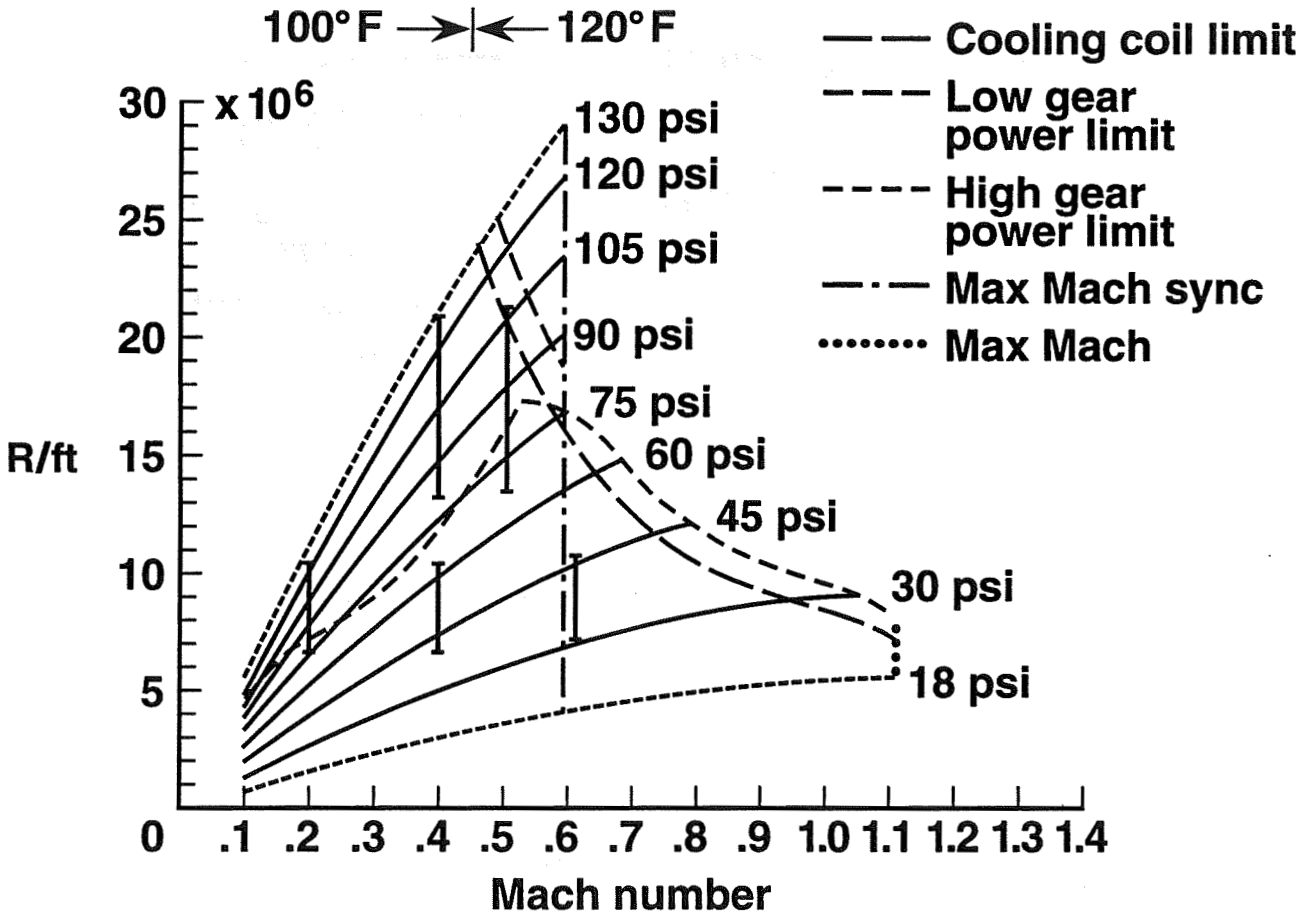
Figure 11: Proposed test plan for the NTF 10^0-cone. Nitrogen mode at ambient temperature, runs 22 through 24 (lower three bars), and air mode at ambient temperature, runs 25 and 26 (upper two bars).
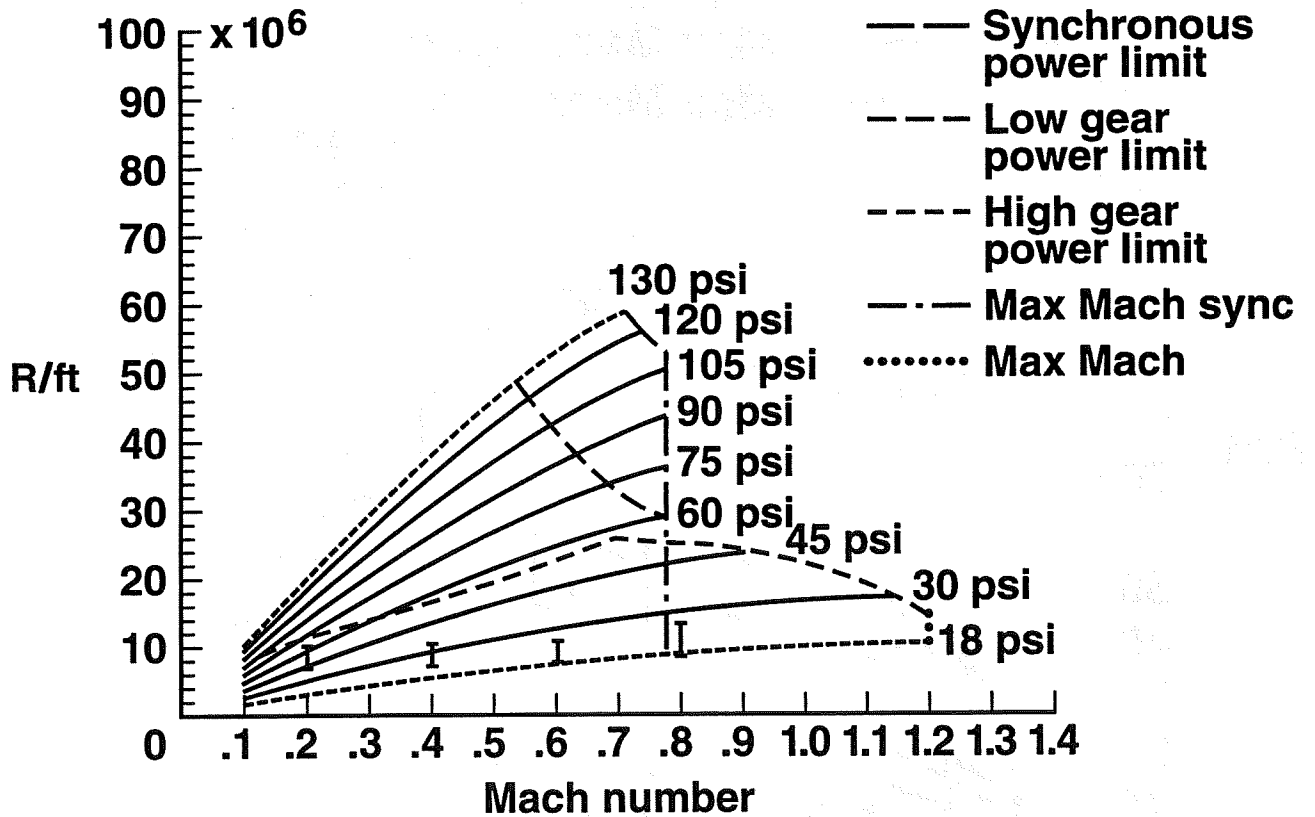
Figure 12: Proposed test plan for the NTF 10^0-cone. Nitrogen mode at -100^0 F, runs 27 through 30.
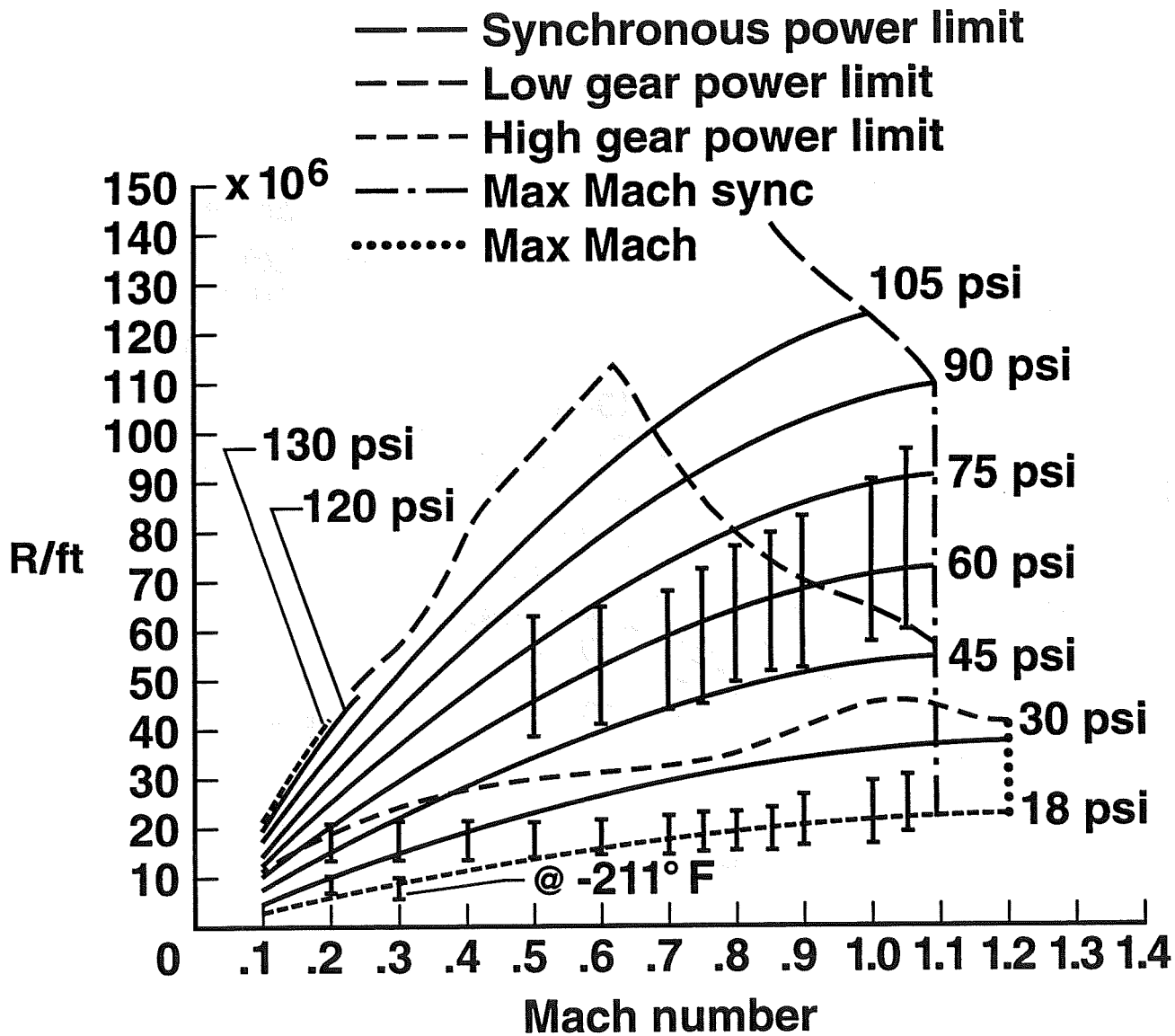
Figure 13: Proposed test plan for the NTF 10^0-cone. Nitrogen mode at -211^0 F and -250^0 F, runs 31 through 53.

REPORT DOCUMENTATION PAGE

1. AGENCY USE ONLY (Leave blank)	2. REPORT DATE	3. REPORT TYPE AND DATES COVERED
	September 1995	Contractor Report(November 1993-August 1995)

4. TITLE AND SUBTITLE

A Concept for Transition Mapping on a 10°-Cone in the National Transonic Facility Using Flow-Pressure Variation

5. FUNDING NUMBERS

NAS1-19858, Task 45

505-59-54-01

6. AUTHOR(S)

Ehud Gartenberg

7. PERFORMING ORGANIZATION NAME(S) AND ADDRESS(ES)

Old Dominion University
Department of Mechanical Engineering
Norfolk, VA 23529-0247

8. PERFORMING ORGANIZATION REPORT NUMBER

9. SPONSORING / MONITORING AGENCY NAME(S) AND ADDRESS(ES)

NASA Langley Research Center
Hampton, VA 23681-0001

10. SPONSORING / MONITORING AGENCY REPORT NUMBER

NASA CR-198209

11. SUPPLEMENTARY NOTES

Langley Technical Monitor: Lawrence E. Putnam

12a. DISTRIBUTION / AVAILABILITY STATEMENT

Unclassified-Unlimited
Subject Category 34

12b. DISTRIBUTION CODE

13. ABSTRACT (Maximum 200 words)

A conceptual study was performed to define a technique for mapping the boundary-layer transition on a 10°-Cone in the National Transonic Facility (NTF) as a means of determining this cryogenic-tunnel suitability for laminar flow testing. A major challenge was to devise a test matrix using a fixed surface-Pitot probe, varying the flow pressure to produce the actual Reynolds numbers for boundary-layer transition. This constraint resulted from a lack of a suitable and reliable electrical motor to drive the probe along the cone's surface under cryogenic flow conditions.

The initial phase of this research was performed by the author in collaboration with the late Dr. William B. Igoe from the Aerodynamics Division at NASA Langley Research Center. His comments made during the drafting of this document were invaluable and a source of inspiration.

14. SUBJECT TERMS

Boundary-Layer Transition, 10°-Cone, Laminar-Flow Testing, Cryogenic Wind Tunnels

15. NUMBER OF PAGES

49

16. PRICE CODE

A03

17. SECURITY CLASSIFICATION OF REPORT	18. SECURITY CLASSIFICATION OF THIS PAGE	19. SECURITY CLASSIFICATION OF ABSTRACT	20. LIMITATION OF ABSTRACT
Unclassified	Unclassified	Unclassified	Unlimited